

Influence of the oxime and anomeric configurations on the stability of 2-deoxy-2-hydroxyimino-D-hexopyranosides



Magdalena Cyman^a, Justyna Wielińska^a, Henryk Myszka^a, Damian Trzybiński^b, Artur Sikorski^a, Andrzej Nowacki^a, Beata Liberek^{a,*}

^a Faculty of Chemistry, University of Gdańsk, Wita Stwosza 63, 80-308 Gdańsk, Poland

^b Biological and Chemical Research Centre, University of Warsaw, Żwirki i Wigury 101, 02-089 Warsaw, Poland

ARTICLE INFO

Article history:

Received 27 April 2016

Received in revised form

5 July 2016

Accepted 8 July 2016

Available online 9 July 2016

Keywords:

Oximes of hex-2-ulopyranosides

Oxime isomerization

Conformation

Exo-anomeric effect

DFT calculations

Single-crystal

ABSTRACT

The *Z/E* isomerisations of the synthesized benzyl 3,4,6-tri-*O*-acetyl-2-deoxy-2-hydroxyimino-*D*-hexopyranosides during the NMR measurement and during the Zemplén *O*-deacetylation were observed. In order to study stabilities and tendency of the obtained compounds to isomerise, B3LYP/6-311++G** level geometry optimisations for four stereoisomers of methyl 2-deoxy-2-hydroxyimino-*D*-*arabino*-hexopyranosides in both the *O*-acetylated and *O*-deacetylated forms were performed. The results of our theoretical studies are fully in agreement with the experimental data and NMR analysis. Additionally, a single-crystal X-ray diffraction data for benzyl 2-deoxy-2-hydroxyimino- α -*D*-*lyxo*-hexopyranoside are reported to supplement our theoretical studies.

© 2016 Elsevier B.V. All rights reserved.

1. Introduction

2-Deoxy-2-hydroxyimino-hexopyranosides, also called oximes of hex-2-ulopyranosides, are useful intermediates in sugar synthesis, which have been applied for a long time [1–3]. Their usefulness stems from the fact that these compounds are easily transformed into different sugar derivatives. Thus, nucleophilic substitution of the allylic 3-*O*Ac group in acetylated 2-deoxy-2-hydroxyimino glycosides with azide or hydride ions affords 3-azido-3-deoxy or 3-deoxy derivatives, respectively (pathway **A**, Scheme 1) [4,5]. In turn, reduction of the 2-hydroxyimino group is the straightforward way for the preparation of 2-amino-2-deoxy sugars (pathway **B**) [6]. The latter transformation was successfully applied to the synthesis of 2-*N*Ac oligosaccharides [7,8] as well as aminoglycoside antibiotics [9–11]. Most importantly, reduction of the oxime is strongly stereospecific and provides mainly 1,2-*cis* 2-amino-2-deoxy glycosides [12–16].

Hydroxyimino function is also used to obtain 2-uloses by deoxygenation with acetaldehyde/HCl (pathway **C**) [5,17,18]. The 2-

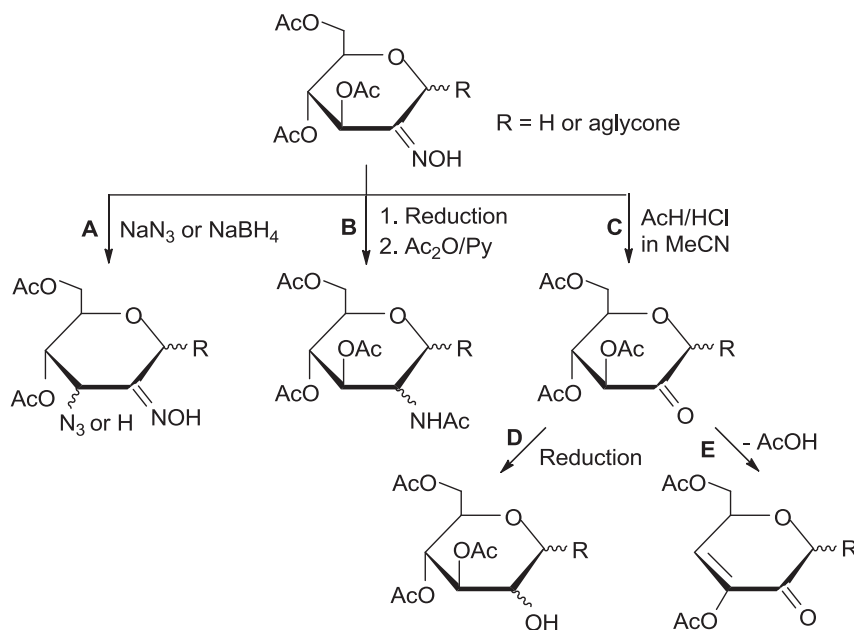
oxo group is easily reduced to the 2-hydroxyl group (pathway **D**) with a high preference for the respective β -*D*-mannosides when β -hex-2-ulopyranosides with *D*-*arabino* configuration are reduced by borohydride reagents [3]. In turn, the 3,4-elimination of acetic or benzoic acid from 2-uloses, such as *O*-protected 1,5-anhydro-*D*-fructoses, provides the pyranoid enolone esters (pathway **E**). A variety of synthetically useful additions are carried out with these esters with high selectivity [19].

Different methodologies have been applied to synthesise 2-deoxy-2-hydroxyimino glycosides. Lemieux introduced a very useful reaction of acetyl-protected 2-deoxy-2-nitroso- α -*D*-glycopyranosyl chlorides with the respective glycosyl acceptor to obtain 2-deoxy-2-hydroxyimino glycosides [1]. In turn, Lichtenthaler proposed the reaction of benzoyl-protected 2-deoxy-2-hydroxyimino- α -glycopyranosyl bromides with the respective glycosyl acceptor [2]. The same goal was achieved in the reaction of respective ulosyl bromide with a glycosyl acceptor followed by oximation of the ketone group [20]. Hex-2-ulopyranoside oximes were also obtained from the previously prepared ulosides [21] and in the reaction of methyl 3,4,6-tri-*O*-acetyl-2-bromo-2-deoxy- β -*D*-glucopyranoside with sodium cobaloxime followed by photolysis in the presence of nitrous oxide [12].

2-Deoxy-2-hydroxyimino glycosides are found in four

* Corresponding author.

E-mail address: beata.liberek@ug.edu.pl (B. Liberek).



Scheme 1. Possible transformations of 3,4,6-tri-*O*-acetyl-2-deoxy-2-hydroxyimino sugars.

stereoisomeric forms. These are α or β glycosides with *Z* or *E* configurations of the oxime (Fig. 1). The ratio of stereoisomers obtained depends on the method used as well as on the stability of a particular stereoisomer.

In a search of new effective inhibitors of GlcN-6P synthase, the enzyme proposed as a target for antifungal chemotherapy [22], we paid attention to 2-deoxy-2-hydroxyimino sugars. The 2-hydroxyimino group mimics the 2-imino group present in the putative reaction intermediate proposed for the reaction catalysed by GlcN-6P synthase [23]. This prompts the assumption that the 2-deoxy-2-hydroxyimino alditols may act as GlcN-6P synthase inhibitors and consequently as antifungal agents. In order to obtain such the compounds we first synthesized benzyl 3,4,6-tri-*O*-acetyl-2-deoxy-2-hydroxyimino-*D*-hexopyranosides with *D*-*arabino* and *D*-*lyxo* configurations, which were next *O*-deacetylated. Undesirable changes of the 2-hydroxyimino group configuration during the experiments prompted us to study the influence of the anomeric carbon and oxime configurations on the stability of 2-deoxy-2-hydroxyimino glycosides. Oximes are known to undergo reversible *E/Z* isomerization due to the relatively low transition states connecting both isomers. However, some of the oxime isomers are isolable species with good stability. On the other hand, both the

anomeric carbon and oxime configurations can be crucial for pharmacological properties and reactivity of the synthesized compounds [24]. Therefore, it seems to be reasoned to well understand tendency of 2-uloside oximes to isomerise. Importantly, our theoretical studies are verified with the presented experimental data. It is worthy to notice that the *E/Z* oxime isomerization in 2-(hydroxyimino)-2-phenylacetonitrile have been recently investigated by spectroscopic and theoretical methods [25].

Calculations were performed using DFT methods at the B3LYP/6-311++G** level for methyl 2-deoxy-2-hydroxyimino-*D*-*arabino*-hexopyranosides in both the *O*-acetylated and *O*-deacetylated forms. To simplify calculations, the methyl glycoside was used instead of the benzyl glycoside. We assume that this does not change a general tendency concerning the stability of 2-deoxy-2-hydroxyimino-*D*-hexopyranosides. Additionally, a single-crystal X-ray diffraction analysis for benzyl 2-deoxy-2-hydroxyimino- α -*D*-*lyxo*-hexopyranoside is reported. This improves the geometry studies presented on 2-deoxy-2-hydroxyimino glycosides.

2. Results and discussion

2.1. Synthesis and NMR investigations

Starting from 3,4,6-tri-*O*-acetyl-2-deoxy-2-nitrosohexopyranosyl chlorides with α -*D*-gluco (1) and α -*D*-galacto (2) configurations, we synthesized benzyl 3,4,6-tri-*O*-acetyl-2-deoxy-2-hydroxyimino-*D*-hexopyranosides with *D*-*arabino* (3–5) and *D*-*lyxo* (6–8) configurations (Scheme 2). Both of the glycosylations provide a mixture of products, which were separated. Thus, the reaction of 1 with benzyl alcohol yields glycosides with β -*E* (3, 9%), α -*Z* (4, 46%), and β -*Z* (5, 8%) configurations of the anomeric carbon and oxime. Compound 5 isomerises to 3 during the NMR measurement in CDCl₃ to generate a mixture of 5 and 3 in a ratio of 1:2, estimated from the NMR spectrum. In turn, the reaction of 2 with benzyl alcohol yields a mixture of glycosides with β -*E* (6) and β -*Z* (7) configurations (11%) in a ratio of 1:2 estimated from the NMR spectrum, and glycoside with the α -*Z* configuration (8, 43%).

Geometries of the synthesized glycosides were established on the basis of NMR spectra. Thus, the H1 signals of 4 and 8 (δ 6.09 and

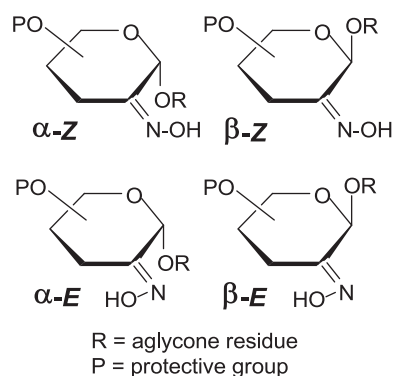
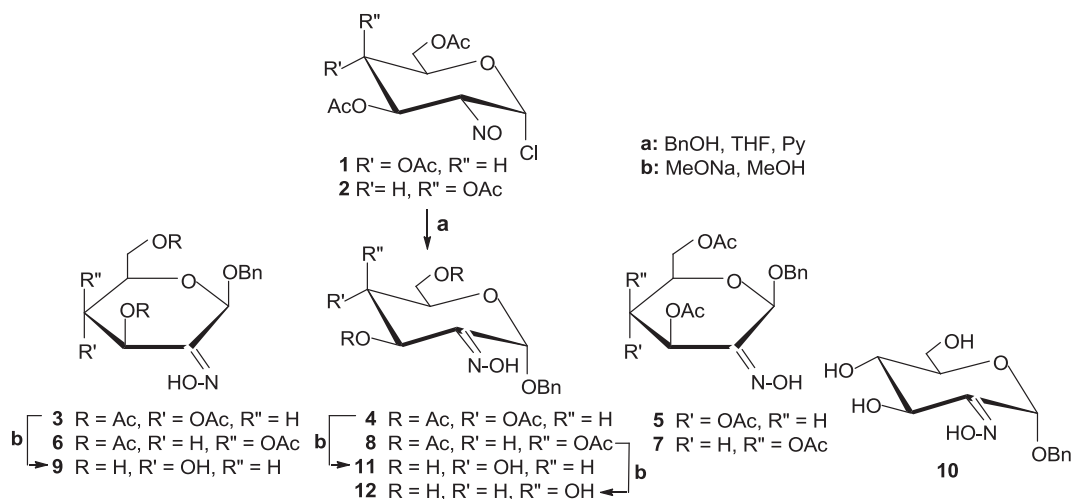


Fig. 1. Stereoisomeric forms of 2-deoxy-2-hydroxyimino glycosides.



Scheme 2. Synthesis of benzyl 3,4,6-tri-O-acetyl-2-deoxy-2-hydroxyimino-D-hexopyranosides and their O-deacetylation.

6.17, respectively) appear at higher δ values than those of the analogous protons of **3**, **5**, **6** and **7** (δ 5.23, 5.89, 5.19 and 5.79, respectively). This is the result of equatorial orientations of the H1 proton corresponding to the α configuration in **4** and **8**. Additionally, the hydroxyl pointed toward the H1 proton (the *Z* configuration) causes its deshielding [5]. In turn, the H3 signals of **3** (δ 6.12), and **6** (δ 6.32) indicate the *E* geometry of the oxime, since the hydroxyl pointed toward the H3 proton causes its distinct deshielding. The H3 proton signals of **4** (δ 5.82), **5** (δ 5.54), **7** (δ 5.73) and **8** (δ 5.90) are due to the *Z* orientation of the 2-hydroxyimino group.

Analysis of the coupling constants reveals that the α -*Z*-D-*arabino* glycoside (**4**) with $J_{3,4}$ 9.65 Hz and $J_{4,5}$ 9.8 Hz as well the α -*Z*-D-*lyxo* glycoside (**8**) with $J_{3,4}$ 3.4 Hz adopt the 4C_1 conformation. A lack of coupling between the H4 and H5 protons is additional proof of the 4C_1 conformation of **8** [26]. Examination of the analogous coupling constants of β -*E*-D-*arabino* glycoside **3** ($J_{3,4}$ 7.4 Hz, $J_{4,5}$ 8.8 Hz), β -*Z*-D-*arabino* glycoside **5** ($J_{3,4}$ 5.5 Hz, $J_{4,5}$ 5.5 Hz), β -*E*-D-*lyxo* glycoside **6** ($J_{3,4}$ 3.9 Hz, $J_{4,5}$ 4.65 Hz) and β -*Z*-D-*lyxo* glycoside **7** ($J_{3,4}$ 3.35 Hz, $J_{4,5}$ 5.8 Hz) calls for the conformations other than 4C_1 . The chair form is probably strongly destabilised in the case of β glycosides owing to the steric and electronic interactions between the nearly coplanar aglycone, oxime and 3-OAc group, both in the *Z* and *E* geometry. Such unfavourable interactions usually cause adoption of a conformation other than 4C_1 [20,27].

Conventional Zemplén O-deacetylation of benzyl 3,4,6-tri-O-acetyl-2-deoxy-2-hydroxyimino-D-hexopyranosides with β -*E*-*arabino* (**3**) and α -*Z*-*lyxo* (**8**) configurations provided the respective 2-deoxy-2-hydroxyimino-D-hexopyranosides (**9** and **12**) with an unchanged oxime configuration. Unexpectedly, analogous O-deacetylation of **4** (α -*Z*-*arabino* configuration) led to two products. The first was 2-hydroxyimino glycoside with the α -*E*-*arabino* configuration (**10**) and the second was 2-hydroxyimino glycoside with the α -*Z*-*arabino* configuration (**11**). Surprisingly, this is relatively stable α -*Z*-*arabino* stereoisomer (**4**) which affords the *E/Z* mixture of O-deacetylated products. Moreover, isolated **10** isomerises to **11** during NMR measurements in CD₃OD, again generating a mixture of **10** and **11** in a ratio of 1:1.14, estimated from the NMR spectrum. It has to be mentioned that changes of the 2-hydroxyimino group configuration were also observed during a Zemplén O-deacetylation of the derivatives of 1,5-anhydrofructoses [28].

Analysis of the coupling constants of 2-deoxy-2-hydroxyimino-D-hexopyranosides with the unprotected hydroxyls reveals that the α -*E*-D-*arabino* glycoside (**10**) with $J_{3,4}$ 9.45 Hz, the α -*Z*-D-*arabino*

glycoside (**11**) with $J_{3,4}$ 9.25 Hz and $J_{4,5}$ 9.6 Hz, as well the α -*Z*-D-*lyxo* glycoside (**12**) with $J_{3,4}$ 3.2 Hz adopts the 4C_1 conformation. Again, a lack of coupling between the H4 and H5 protons is additional proof of the 4C_1 conformation of **12** [26]. Examination of the $J_{3,4}$ 8.4 Hz and $J_{4,5}$ 9.4 Hz coupling constants of the β -*E*-D-*arabino* glycoside **9** is discussed below with the presented calculations (point 2.3).

2.2. DFT studies on methyl 3,4,6-tri-O-acetyl-2-deoxy-2-hydroxyimino-D-*arabino*-hexopyranosides

To reduce a number of generated structures, we anticipated that the methyl group of an aglycone would be oriented antiperiplanar to the C2 carbon atom of the pyranose ring, in both the axial and the equatorial orientations of the methoxy group, as a result of the exo-anomeric and steric effects. This is in agreement with our previously reported findings [29]. In the starting geometries, hydrogen from the =N–OH group was oriented *anti* (a) or *syn* (s) with reference to the C2 carbon atom.

The two conformations were taken into account, i.e. anti-periplanar (a) and synclinal (s), with reference to the AcO3–C3 and AcO4–C4 bond rotations. Of the two possible synclinal conformations, the one with the carbonyl carbon *gauche* oriented to both sugar ring carbon atoms (+*sc*, Fig. 2a and -*sc*, Fig. 2b) was excluded. As previously reported, the OAc group avoids such orientation [30]. With reference to the C6–C5 bond rotations, three staggered conformations were considered, assigned in a common way as *gg*, *gt* and *tg* (Fig. 2c). Three staggered conformations were also considered regarding the AcO6–C6 bond rotations. These were assigned “a” for the *ap* orientation, “s” for the +*sc* orientation and “s” for the -*sc* orientation (Fig. 2d). In turn, one orientation was considered with reference to the CO–O bond rotation in acetyl groups, because, due to the mesomeric effect, the acetoxy group is planar, starting from the respective pyranose carbon atom. Being planar, the acetoxy group strongly prefers the orientation in which the carbonyl oxygen is eclipsed by the respective sugar carbon atom [30].

Thus, by taking into account two orientations of the N–OH group ($\times 2$) as well as a rotational freedom of the 3-OAc, 4-OAc, 6-OAc, and 5-CH₂OAc groups ($2 \times 2 \times 3 \times 3$), 72 starting geometries for α -*Z*, α -*E*, β -*Z*, and β -*E* stereoisomers of methyl 3,4,6-tri-O-acetyl-2-deoxy-2-hydroxyimino-D-*arabino*-hexopyranosides, respectively, were prepared for the calculations. All geometries were prepared in the 4C_1 conformation. To describe the initial and final geometries of the pyranose ring substituents, the following assignments and

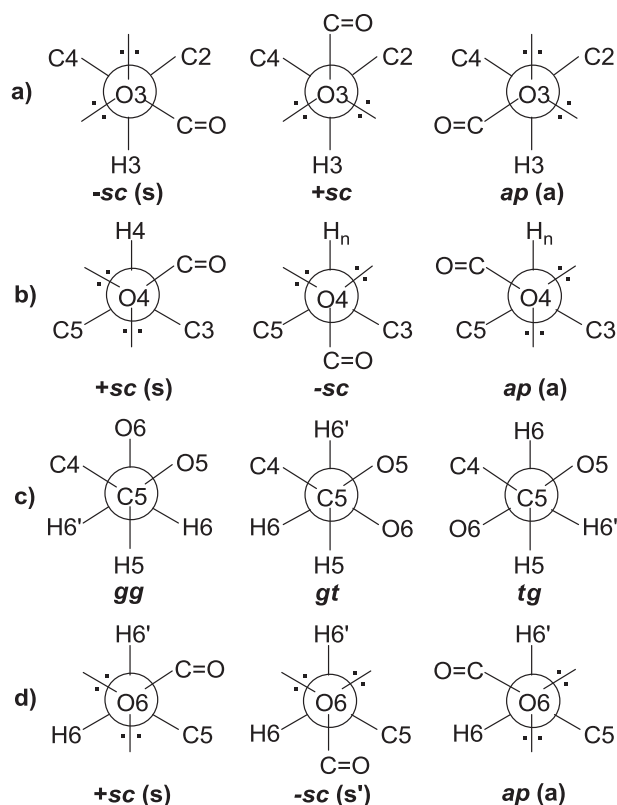


Fig. 2. Newman projections along the (a) O3–C3, (b) O4–C4, (c) C5–C6 and (d) O6–C6 bonds corresponding to the respective geometries of the studied compounds.

orders of rotations were used: N–OH (a or s), O3–C3, O4–C4 (a or s), C6–C5 (gg, gt or tg), and O6–C6 (a, s, or s'). The optimisation procedure reduced the number of geometries since many of them were converted to the same optimised structure. Table 1 lists the geometry and energy parameters of the most stable optimised structures as well as the population of each rotamer in a group of rotamers with the same anomeric and oxime configurations.

The findings presented in Table 1 show that α -Z is the most stable of the four stereoisomers of methyl 3,4,6-tri-*O*-acetyl-2-deoxy-2-hydroxyimino-*D*-arabino-hexopyranosides. Its average energy, calculated between the relatively stable rotamers 1–4, is about 2.5 kcal/mol lower than an analogous energy of the relatively stable rotamers 1–9 of the α -*E* stereoisomer. Probably, due to this energy difference, the α -*E* stereoisomer is not formed in the glycosidation carried out here. The results also indicate that the β -Z and β -*E* stereoisomers are definitely less stable than the α -Z stereoisomer (on average 3.7 kcal/mol and 3 kcal/mol, respectively). Both of these are also less stable than the α -*E* stereoisomer (on average 1.2 kcal/mol and 0.5 kcal/mol, respectively). The relatively small energy difference between the β -*E* and the β -Z stereoisomers justifies the observed 5 (β -Z) \rightarrow 3 (β -*E*) isomerization, which occurs during the NMR measurement in CDCl₃.

As demonstrated, all of the most stable α -Z rotamers (1–4, population of 99.98%) adopt the 4C_1 conformation (Table 1, Fig. 3). The α -Z stereoisomer is stable enough in the 4C_1 conformation since the α -configured aglycone does not show steric hindrance for the Z-configured oxime. Moreover, the 4C_1 conformation of the α -Z stereoisomer allows the oxime oxygen to interact with the equatorially oriented anomeric hydrogen. Such advantageous interaction is possible since the calculated distance between the oxime oxygen and the equatorially oriented anomeric hydrogen in the α -Z stereoisomer (1–4) is 2.31 Å. The equatorially oriented 3-*O*Ac group

shows steric hindrance for the α -*E* stereoisomer in the 4C_1 conformation. Additionally, planar orientation of the O3–C3–C2–N–O sequence of atoms in a case of the α -*E* stereoisomer should cause electronic repulsions between the oxygen atoms. The calculated distance between the oxime and O3 oxygen atoms is 2.7 Å (on average). Such unfavourable interactions in the 4C_1 conformation of the α -*E* stereoisomer cause an increase of energy (about 2.5 kcal/mol, as calculated). These also cause a certain deformation of the 4C_1 conformation. Although the majority of the relatively stable rotamers of the α -*E* stereoisomer adopt the 4C_1 conformation, some of them prefer the 0H_5 conformation. In the case of β anomers of 3,4,6-tri-*O*-acetyl-2-deoxy-2-hydroxyimino-*D*-hexopyranosides, both the Z and *E* configurations are unfavourable. The Z-configured oxime constitutes steric and electronic hindrance for an aglycone in the 4C_1 conformation of β anomers. In turn, the *E*-configured oxime constitutes steric and electronic hindrance for the 3-*O*Ac group in the 4C_1 conformation. Our calculations indicate that these unfavourable interactions are stronger in the case of the β -Z stereoisomer. In both cases, these strains cause a change in the chair conformation. None of the *E* nor Z isomers of β anomers adopt the 4C_1 conformation. As illustrated in Table 1, the β -*E* stereoisomer prefers the ${}^1S_3 \rightleftharpoons {}^1^4B \rightleftharpoons {}^4S_0$ conformational equilibrium. Importantly, the calculations confirm the experimental findings of our group and others [20].

The presented results indicate that all of the stable rotamers of methyl 3,4,6-tri-*O*-acetyl-2-deoxy-2-hydroxyimino-*D*-arabino-hexopyranosides, regardless of their anomeric and oxime configurations, have the hydrogen from the =N–OH group oriented *anti* (a) with reference to the C2 carbon atom. Such an orientation seems to be sterically less strained. Additionally, such an orientation allows the oxime oxygen to interact with the anomeric proton in a case of the α -Z and the β -Z stereoisomers. With reference to the O3–C3 bond rotation, the α -Z stereoisomer solely prefers the +sc (s) orientation, whereas the β -*E* stereoisomer solely prefers the *ap* (a) orientation. In the case of β -Z and α -*E* stereoisomers, both the +sc (s) and *ap* (a) orientations are present among the stable rotamers. It seems that the O4–C4 bond rotation depends on the O3–C3 bond rotation, and *vice versa*. This means that if the O3–C3 bond rotation prefers the +sc (s) orientation, the O4–C4 bond rotation prefers the *ap* (a) orientation. In turn, if the O3–C3 bond rotation prefers the *ap* (a) orientation, the O4–C4 bond rotation prefers the +sc (s) orientation. The C5–C6 and O6–C6 bond rotations have a relatively small influence on the stability of the explored stereoisomers. All of the orientations taken into account with reference to these rotations are present among the stable rotamers.

2.3. DFT studies on methyl 2-deoxy-2-hydroxyimino-*D*-arabino-hexopyranosides

To generate starting structures of 2-deoxy-2-hydroxyimino-*D*-arabino-hexopyranosides, we anticipated, analogously to the previous point, that the methyl group would be oriented in accordance with the *exo*-anomeric effect, i.e. antiperiplanar to the C2 carbon atom of the pyranose ring, in both the axial and the equatorial orientations of the methoxy group. In accordance with the rotational freedom of the 3-OH and 4-OH groups, we considered two orientations, *cw* and *ccw*, with the cooperative arrangement of intramolecular hydrogen bonding-like interactions that is a reasonable approximation [31]. Three low-energy positions of the hydroxymethyl group, in relation to the sugar ring, designated *gg*, *gt* and *tg*, were taken into account (Fig. 2c). Rotation about the C6–O6 bond was not considered. The spatial disposition of the 6-OH hydrogen atom is closely connected to the orientation of the

Table 1
Geometry parameters, energy parameters, and populations of the most stable rotamers of methyl 3,4,6-tri-*O*-acetyl-2-deoxy-2-hydroxyimino-*D*-*arabino*-hexopyranosides.

Structure	Final geometry ^a	Final conformation	ΔE^b [kcal/mol]	G [a.u.]	ΔG^c [kcal/mol]	Population ^d [%]
<i>α-Z</i>						
1	a/s/a-s/gt/a	⁴ C ₁	0.51	-1238.65463	0.00	36.63
2	a/s/a-s/gg/s-a	⁴ C ₁	0.00	-1238.65448	0.09	31.21
3	a/s/a/gt/s	⁴ C ₁	0.48	-1238.65434	0.18	26.88
4	a/s/a/tg/s	⁴ C ₁	1.22	-1238.65280	1.15	5.26
						ΣP_i 99.98
<i>α-E</i>						
1	a/s/a-s/gt/a	⁴ C ₁	2.75	-1238.65056	0.00	25.42
2	a/s/a-s/gg/a-s	⁴ C ₁	2.29	-1238.65040	0.10	21.34
3	a/s/a/gt/s	⁴ C ₁	2.73	-1238.65035	0.14	20.20
4	a/a/s/gt/s	⁰ H ₅	3.82	-1238.64986	0.44	12.03
5	a/a/s/gg/a	⁰ H ₅	3.15	-1238.64945	0.70	7.82
6	a/a/s/gt/a	⁰ H ₅	3.35	-1238.64895	1.01	4.60
7	a/s/a/gt/s	⁴ C ₁	2.74	-1238.64878	1.12	3.84
8	a/s/a/tg/a	⁴ C ₁	3.74	-1238.64836	1.38	2.45
9	a/s/a/tg/s	⁴ C ₁	3.42	-1238.64802	1.60	1.72
						ΣP_i 99.42
<i>β-Z</i>						
1	a/s/a-s/gt/s-a	¹ S ₃	4.07	-1238.64805	0.00	26.87
2	a/a-s/a-s/gg/a-s	^{1,4} B _{def}	4.18	-1238.64785	0.13	21.74
3	a/s/a/gt/s	⁴ S ₀	4.06	-1238.64783	0.14	21.10
4	a/s/a-s/tg/a	⁴ S ₀	4.67	-1238.64764	0.26	17.27
5	a/a/s/gg/a	^{1,4} B _{def}	4.30	-1238.64717	0.55	10.58
6	a/s/a-s/tg/s	⁴ S ₀	5.78	-1238.64516	1.82	1.25
						ΣP_i 98.81
<i>β-E</i>						
1	a/a/s/gg/a	^{1,4} B _{def}	2.82	-1238.65013	0.00	48.13
2	a/a/s/gg/a-s	^{1,4} B _{def}	2.63	-1238.6494	0.46	22.30
3	a/a/a-s/tg/s	^{1,4} B _{def}	3.42	-1238.64825	1.18	6.59
4	a/a/a/tg/a	^{1,4} B _{def}	4.59	-1238.64813	1.26	5.76
5	a/a-s/a/gt/s	^{1,4} B _{def}	4.13	-1238.64793	1.38	4.68
6	a/a/s/gt/s	^{1,4} B _{def}	3.41	-1238.6478	1.46	4.07
7	a/a/s/gt/s	^{1,4} B _{def}	4.41	-1238.64764	1.56	3.44
8	a/a/a/tg/a	^{1,4} B _{def}	4.58	-1238.64748	1.66	2.90
9	a/a/a/tg/s	^{1,4} B _{def}	4.83	-1238.64693	2.01	1.63
						ΣP_i 99.50

^a The sign “-” indicates that conformation is in-between the left one and the right one.

^b With reference to the rotamer **2** (*α -Z*) with energy of -1238.923254 a.u.

^c With reference to the most stable rotamer with the same anomeric and oxime configurations.

^d In rotamers with the same anomeric and oxime configurations.

hydroxymethyl group and the *ccw/cw* arrangement of the 3-OH and 4-OH groups. In the *gg* and *gt* orientations, the 6-OH hydrogen atom is directed towards the O5 oxygen atom, regardless of the *ccw/cw* arrangement. In the *tg* orientation, the 6-OH hydrogen atom is oriented towards the O4 oxygen atom in the *ccw* arrangement of the 3-OH and 4-OH groups, forming an intramolecular hydrogen bond. In the *cw* arrangement, the 4-OH hydrogen atom forms an intramolecular hydrogen bond with the O6 oxygen. In the starting geometries, hydrogen atom from the =N-OH group was oriented *anti* (a) or *syn* (s) with reference to the C2 carbon atom.

By taking into account two orientations of the N-OH group ($\times 2$), *ccw* and *cw* orientations of the 3-OH and 4-OH groups ($\times 2$), and rotational freedom of the CH₂OH group ($\times 3$), 12 starting geometries for *α -Z*, *α -E*, *β -Z*, and *β -E* stereoisomers of methyl 2-deoxy-2-hydroxyimino-*D*-*arabino*-hexopyranosides were prepared. All of the starting geometries were prepared in both the chair (⁴C₁) and the skew (⁴S₀) conformations. To describe initial and final geometries of the pyranose ring substituents the following assignments and orders of rotations were used: NO-H (a or s), O3-C3, O4-C4 (*cw* or *ccw*), C6-C5 (*gg*, *gt* or *tg*).

The findings presented in Table 2 demonstrate that among the four stereoisomers of methyl 2-deoxy-2-hydroxyimino-*D*-*arabino*-hexopyranosides, the *α -Z* is again the most stable. However, the acetyl group deprotection causes the energy difference between the *α -Z* and *α -E* stereoisomers to decrease. The most stable

rotamers of the *α -E* stereoisomer (**1–3**) are on average 1.7 kcal/mol less stable than the most stable rotamers of the *α -Z* stereoisomer (**1–3**). The analogous difference in the case of acetylated compounds is 2.5 kcal/mol. Taking into account the acidic properties of oximes (pK_a 11) [32] one may expect that these exist in their anionic form in the strong basic conditions of Zemplén *O*-deacetylation. On the other hand, the anionic form of oximes is characteristic by the lower *E/Z* transition state [25]. This fact as well as the decreased energy difference between the *α -Z* and *α -E* stereoisomers of deacetylated oximes justify the observed **4** (*α -Z*) \rightarrow **10** (*α -E*) + **11** (*α -Z*) isomerization during the Zemplén *O*-deacetylation. In turn, it is not surprising that the less stable **10** (*α -E*) isomerises to the more stable **11** (*α -Z*) during NMR measurements.

The DFT results also indicate that after the acetyl groups removing, the *β -Z* and *β -E* stereoisomers are still definitely less stable than their *α* equivalents. The *β -E* stereoisomer is 2.2 kcal/mol less stable than the *α -E* stereoisomer on average; however, this is about 1.1 kcal/mol more stable than the *β -Z* stereoisomer. Probably, this better stability of the *β -E* stereoisomer over the *β -Z* stereoisomer inhibits the *E/Z* isomerization of **9** during NMR measurements.

The stabilities of the studied methyl hex-2-ulopyranoside oximes are again closely connected with their conformations. The unstrained *α -Z* stereoisomer adopts the ⁴C₁ conformation, which is confirmed by the calculated 99.94% population of the rotamers **1–3**

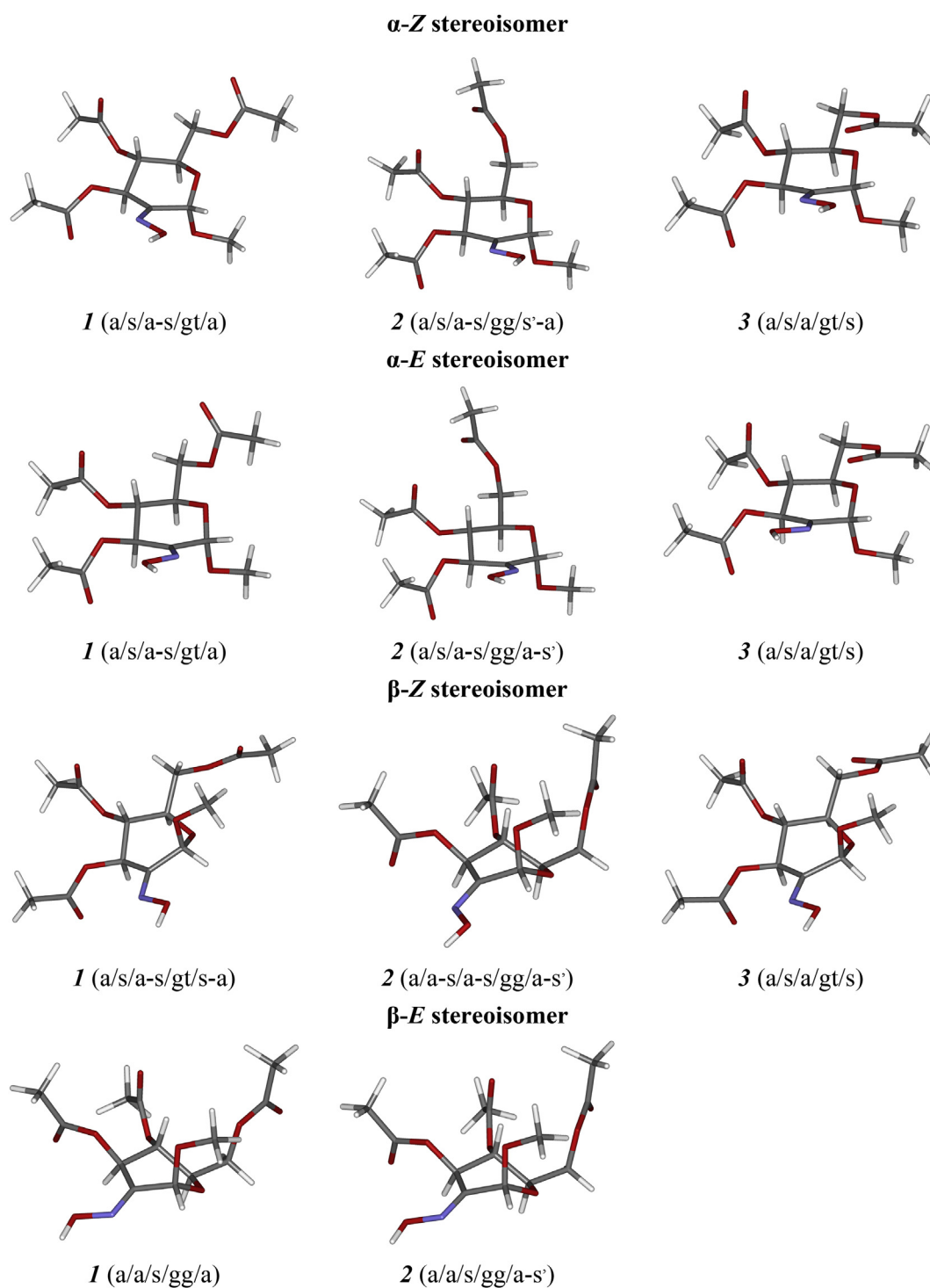


Fig. 3. Structures of the most stable methyl 3,4,6-tri-*O*-acetyl-2-deoxy-2-hydroxyimino-*D*-arabino-hexopyranosides from each group of the configurational isomers.

(Table 2). The α -E stereoisomer also adopts the 4C_1 conformation, which is confirmed by the calculated 99.55% population of the rotamers **1–3**. It seems that the 4C_1 conformation facilitates the 3-OH group hydrogen of the α -E stereoisomer to interact with the oxime oxygen. The distance between these two atoms in the optimised structures **1–3** is 1.86 Å, 1.86 Å, and 1.87 Å, respectively. The strains resulting from the coplanar orientation of the aglycone, oxime and 3-OH groups in the 4C_1 conformation lead the β anomers to adopt other conformations. The most stable rotamers of the β -Z

stereoisomer adopt the deformed $B_{3,0}$ conformation (**6**, population 39%) or the 4S_0 conformations (**7** and **8**, populations 29.86% and 12.71%, respectively). There are also relatively stable 4C_1 conformations found among the β -Z stable rotamers with populations of 7.54% (**1**), 6.22% (**2**) and 3.65% (**3**). These results indicate the conformational equilibrium for the β -Z stereoisomer. In turn, the β -E stereoisomer adopts the deformed 14B conformation, which is proved by the calculated 99.27% population of the rotamers **4–7**. The 14B conformation allows the β -E stereoisomer to avoid the

Table 2
Geometry parameters, energy parameters, and populations of the most stable rotamers of methyl 2-deoxy-2-hydroxyimino-D-arabino-hexopyranosides.

Structure	Final geometry	Final conformation	ΔE^a [kcal/mol]	G [a.u.]	ΔG^b [kcal/mol]	Population ^c [%]	ΔG^d [kcal/mol]	Population ^e [%]
α-Z								
starting chair								
1	a/ccw/gg	4C_1	0.02	-780.640737	0.00	40.43	0.00	40.43
2	a/ccw/gt	4C_1	0.00	-780.640731	0.004	40.17	0.004	40.17
3	a/ccw/tg	4C_1	0.08	-780.640041	0.44	19.34	0.44	19.34
						ΣP_i 99.94		ΣP_i 99.94
starting skew								
4	a/ccw/gt	$B_{3,0}$	7.99	-780.628876	0.00	89.80	7.44	1.41E-04
5	a/ccw/tg	$B_{3,0}$	9.73	-780.626420	1.54	6.65	8.98	1.04E-05
6	s/ccw/gt	$B_{3,0}$ def	9.86	-780.625203	2.30	1.83	9.75	2.87E-06
7	s/ccw/gg	$B_{3,0}$ def	10.35	-780.624877	2.51	1.30	9.95	2.03E-06
						ΣP_i 99.58		ΣP_i 1.56E-04
α-E								
starting chair								
1	a/ccw/tg	4C_1	1.75	-780.638632	0.00	43.96	0.00	43.96
2	a/ccw/gt	4C_1	1.68	-780.638486	0.09	37.66	0.09	37.66
3	a/ccw/gg	4C_1	1.64	-780.637786	0.53	17.93	0.53	17.93
						ΣP_i 99.55		ΣP_i 99.55
starting skew								
4	a/ccw/gt	${}^{1,4}B$ def	8.65	-780.627165	0.00	99.98	7.20	2.32E-04
β-Z								
starting chair								
1	s/ccw/gt	4C_1	5.11	-780.631957	0.00	42.08	0.97	7.54
2	s/ccw/gg	4C_1	5.25	-780.631775	0.11	34.70	1.09	6.22
3	s/ccw/tg	4C_1	4.90	-780.631273	0.43	20.38	1.40	3.65
4	a/ccw/gt	4C_1	7.77	-780.628615	2.10	1.22	3.07	0.22
5	a/ccw/gg	4C_1	7.73	-780.628604	2.10	1.20	3.08	0.22
						ΣP_i 99.58		ΣP_i 17.85
starting skew								
6	a/ccw/gg	$B_{3,0}$ def	4.18	-780.633508	0.00	47.51	0.00	39.00
7	a/ccw/gt	4S_0	5.08	-780.633256	0.16	36.37	0.16	29.86
8	a/ccw/tg	4S_0	5.39	-780.632450	0.66	15.48	0.66	12.71
						ΣP_i 99.36		ΣP_i 81.57
β-E								
starting chair								
1	a/ccw/tg	4C_1 def	6.80	-780.629693	0.00	44.84	2.96	0.23
2	a/ccw/gg	4C_1	7.03	-780.629666	0.02	43.58	2.98	0.22
3	a/ccw/gt	4C_1	7.13	-780.628407	0.81	11.48	3.77	5.80E-2
						ΣP_i 99.90		ΣP_i 0.51
starting skew								
4	a/ccw/gt	${}^{1,4}B$ def	3.85	-780.634410	0.00	33.74	0.00	33.57
5	a/ccw/gg	${}^{1,4}B$ def	3.40	-780.634255	0.10	28.63	0.10	28.49
6	a/ccw/tg	${}^{1,4}B$	3.67	-780.634185	0.14	26.58	0.14	26.45
7	a/ccw/gg	${}^{1,4}B$ def	4.70	-780.633336	0.67	10.81	0.67	10.76
						ΣP_i 99.76		ΣP_i 99.27

^a With reference to the rotamer **2** (α -Z) with energy of -780,8167023 a.u.

^b With reference to the most stable rotamer with the same anomeric and hydroxyimino configurations and the same starting conformation.

^c In rotamers with the same anomeric and oxime configurations and the same starting conformation.

^d With reference to the most stable rotamer with the same anomeric and hydroxyimino configurations, irrespective of its conformation.

^e In rotamers with the same anomeric and oxime configurations, irrespective of their conformation.

unfavourable coplanar orientation of the aglycone, oxime and 3-OH group.

The calculations presented are fully in agreement with our experimental findings, based on the NMR data. Both, presented coupling constants and results of the optimisation call for the 4C_1 conformation of the α -E (**10**) and α -Z (**11**) stereoisomers of methyl 2-deoxy-2-hydroxyimino-D-arabino-hexopyranosides. In turn, the coupling constants established for the β -E diastereoisomer (**9**) is indicative of the deformed ${}^{1,4}B$ conformation, found during the optimisation process. The ${}^{1,4}B$ conformation, analogously to the 4C_1 conformation, requires the H3 and H4 as well as the H4 and H5 protons to be oriented antiperiplanar. Thus, the recorded $J_{3,4}$ 8.4 Hz and $J_{4,5}$ 9.6 Hz coupling constants confirm the deformed ${}^{1,4}B$ conformation calculated for **9**.

With reference to the geometry of pyranose ring substituents, one may see that all of the most stable rotamers of methyl 2-deoxy-2-hydroxyimino-D-arabino-hexopyranosides adopt the ccw

orientation of the 3-OH and 4-OH groups. Such an orientation directs the hydrogen from the 4-OH group towards the oxygen from the 3-OH group and the hydrogen from the 3-OH group towards the nitrogen from the 2=NOH group (in the Z configuration) or towards the oxygen from the 2=NOH group (in the E configuration). In the case of Z configuration, the oxygen from the 2=NOH group is subsequently directed towards the anomeric hydrogen, in both the α and β anomers. Such an orientation is unavoidable for the α anomer in the 4C_1 conformation. In the case of β anomer, the oxygen from the 2=NOH group may interact with the anomeric hydrogen since the most stable rotamers of the β -Z stereoisomer (**6**–**7**) adopt a conformation other than the 4C_1 one (Fig. 4).

Thus, the continuous network of the attractive electronic interactions is created in all of the stable rotamers of methyl 2-deoxy-2-hydroxyimino-D-arabino-hexopyranosides. To make this possible, the hydrogen from the 2=NOH group adopts the *anti* (a) orientation with reference to the C2 carbon atom.

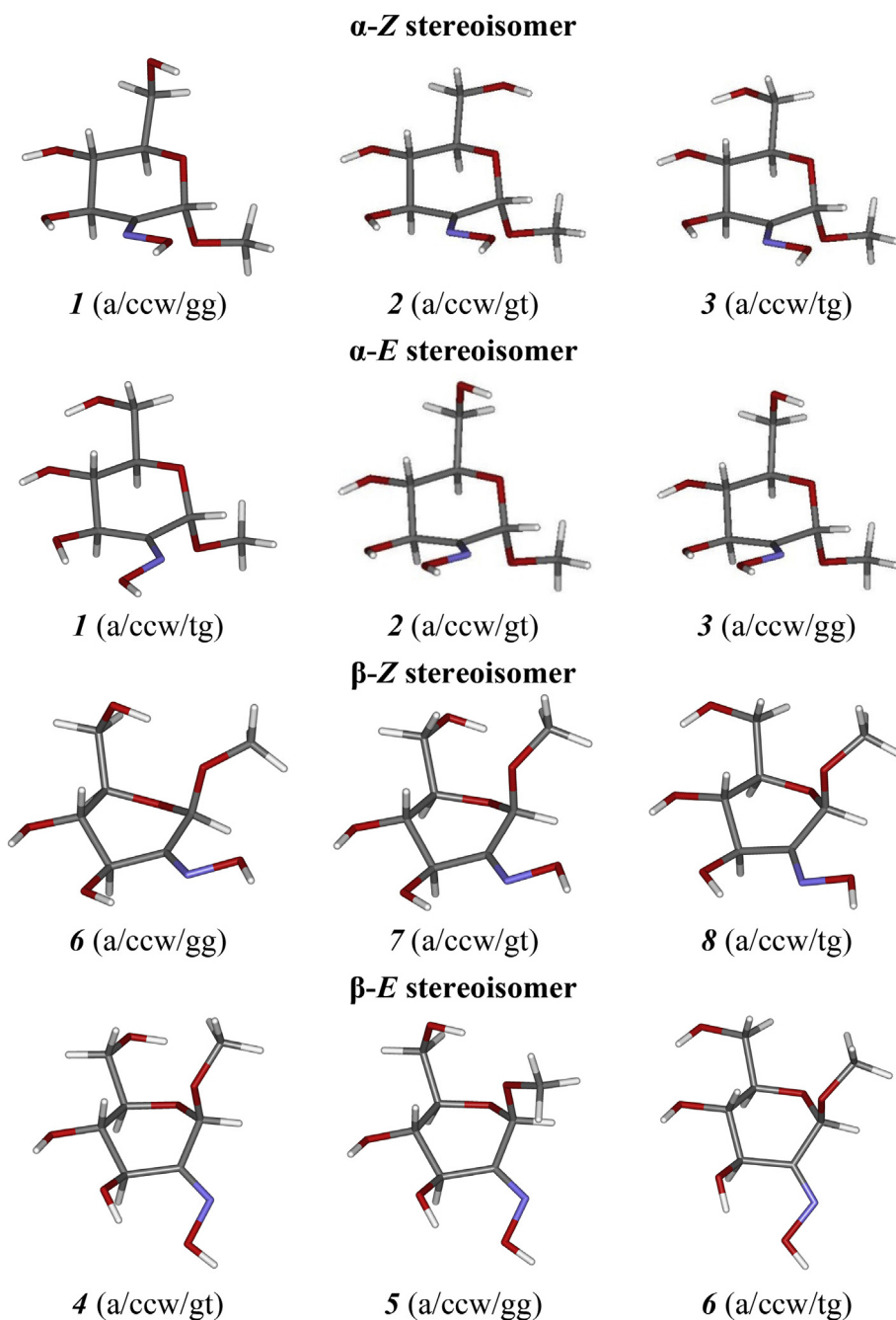


Fig. 4. Structures of the most stable methyl 2-deoxy-2-hydroxyimino-D-arabino-hexopyranosides from each group of the configurational isomers.

The only structural differentiation in the stable rotamers of the respective stereoisomer of methyl 2-deoxy-2-hydroxyimino-D-arabino-hexopyranosides results from the C6–C5 bond rotation. All three permitted staggered orientations (*gg*, *gt*, *tg*, Fig. 2c) are represented among these stable rotamers without any specific preference.

It is worth noticing that in all of the optimised structures, both acetylated and deacetylated, the methyl group of aglycone is always oriented in accordance with an *exo*-anomeric effect, e.g. anti-periplanar to the C2 carbon atom. The only exception is structure 5 of the β -E stereoisomer of methyl 2-deoxy-2-hydroxyimino-D-arabino-hexopyranosides (Fig. 4). In this structure, the methyl group of aglycone is oriented against an *exo*-anomeric effect, e.g.

anti-periplanar to the endocyclic oxygen atom. Such an unfavourable aglycone orientation is probably compensated by a hydrogen bond created between the *gg* oriented 6-OH group and the aglycone oxygen. The 6-OH...OME distance 2.07 Å and the O–H...O valence angle 145.96° give evidence for such the hydrogen bond. Another relatively stable structure of the β -E stereoisomer with the *gg* oriented 6-OH group (7, Table 2) has the methyl group of aglycone oriented in accordance with the *exo*-anomeric effect.

2.4. X-ray analysis of benzyl 2-deoxy-2-hydroxyimino- α -D-lyxo-hexopyranoside (12)

In the crystal, 2-deoxy-2-hydroxyimino- α -D-lyxo-

hexopyranoseide (**12**) adopts the 4C_1 conformation [33,34] (Fig. 5) with the ring-puckering parameters [35,36] $Q = 0.5528(15)$ Å, $\theta = 14.47(15)$ Å and $\phi = 260.1(6)^\circ$. As it was established above, the 4C_1 conformation is stable enough for all of the analysed 2-deoxy-2-hydroxyimino glycosides with the α -Z configuration and was also identified for **12** in a $CDCl_3$ solution.

In a crystal structure of **12** the C7 carbon atom of aglycone is oriented antiperiplanar to the C2 sugar carbon atom with the C7–O1–C1–C2 torsional angle of $169.2(1)^\circ$. Such an orientation is due to an *exo*-anomeric effect and is in accordance with our results of the DFT calculations. In turn, the oxime hydrogen is oriented *anti* with reference to the C2 sugar carbon atom, which is also in accordance with our geometry optimisation results. In a crystal structure of **12** the 3-OH hydrogen is oriented towards the C4 carbon atom with the H3B–O3–C3–C4 torsion angle of $85.2(1)^\circ$. In turn, the 4-OH hydrogen is almost eclipsed with the H4 hydrogen, which is indicated by the H4B–O4–C4–H4A torsion angle of $-8.8(1)^\circ$. The hydroxymethyl group adopts the *tg* conformation with the 6-OH hydrogen pointed to the 4-OH oxygen.

The crystal structure of **12** is stabilised by a dense network of O–H \cdots O hydrogen bonds and C–H \cdots O short contacts between the molecules (Fig. 6). There is also an intramolecular short contact between the Z oriented oxime oxygen and the H1 anomeric proton in the crystal structure of **12**. The distance between these two atoms is 2.22 Å (Table 3). This confirms our assumptions based on the DFT calculations that the α -Z orientation of 2-deoxy-2-hydroxyimino glycosides is also advantageous because of the electronic interactions between the oxime oxygen and the H1 anomeric proton.

3. Conclusions

The results of our experimental and theoretical studies indicate that the α -Z stereoisomer is definitely the most stable among all of the possible stereoisomers of 2-deoxy-2-hydroxyimino-D-hexopyranosides, both in the O-acetylated and O-deacetylated forms. The stability of the remaining stereoisomers decreases in the following order α -E > β -E > β -Z. The α -E stereoisomer relatively gains in stability after O-deacetylation, probably due to the favourable interactions of the 3-OH group with the E-configured oxime oxygen. The 2-hydroxyimino compounds easily isomerises in the direction of the more stable stereoisomer: β -Z to β -E (**5** to **3**) or α -E to α -Z (**10** to **11**). Even the most stable α -Z substrate (**4**) provides the mixture of α -E (**10**) and α -Z (**11**) products in the strong basic conditions of Zamplén deacetylation. This indicates that an

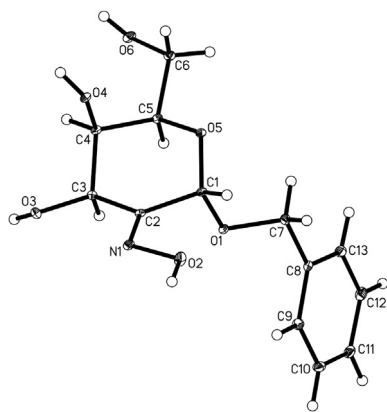


Fig. 5. The molecular structure of **12** showing the atom labelling scheme. Displacement ellipsoids are drawn at the 15% probability level and H atoms are shown as small spheres of arbitrary radius.

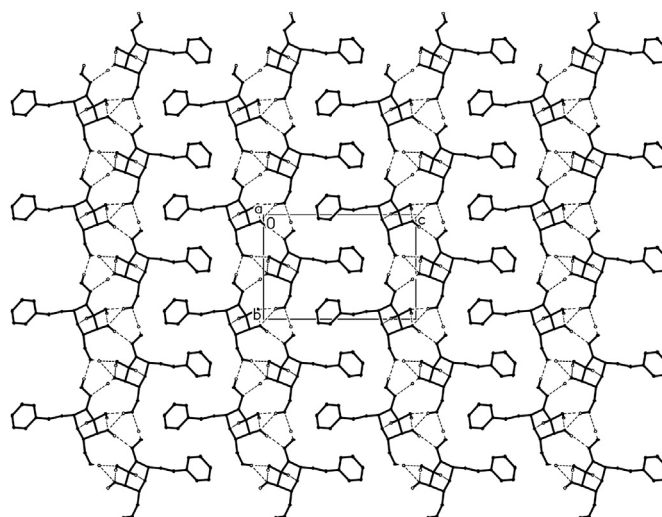


Fig. 6. The arrangement of the molecules of **12** in the crystal structure, viewed along *a*-direction. The O–H \cdots O and C–H \cdots O hydrogen bonds are represented by dashed lines. The H atoms not involved in interactions have been omitted for clarity.

Table 3

Hydrogen bonds and short contacts for **12** with distances (d): $d(D\cdots A) < R(D)+R(A)+0.50$ Å; $d(H\cdots A) < R(H)+R(A)-0.12$ Å and angle (\angle) $\angle D-H\cdots A > 100.0^\circ$.

D–H	A	d(D–H)	d(H \cdots A)	d(D \cdots A)	\angle D–H \cdots A
C-1–H-1	O-2	0.98	2.22	2.636 (2)	104
O-2–H-2	O-6 ⁱ	0.82	1.90	2.719(2)	175
O-3–H-3B	O-4 ⁱⁱ	0.82	2.09	2.902(2)	172
O-4–H-4B	N-1 ⁱⁱⁱ	0.82	2.12	2.912(2)	163
O-6–H-6C	O-3 ⁱⁱⁱ	0.82	1.96	2.737(2)	159
O-6–H-6C	O-4 ⁱⁱⁱ	0.82	2.57	3.079(2)	121
C-3–H-3A	O-5 ⁱⁱ	0.98	2.20	3.144(2)	160

Symmetry codes: (i) $x, y - 1, z$; (ii) $x + 1, y, z$; (iii) $-x, y + 1/2, -z$.

avoidance of basic conditions is important to minimize oxime isomerization. The β anomers lack of stability is closely connected with the fact that these adopt other than 4C_1 conformation. The presented X-ray analysis confirms our experimental and theoretical studies.

4. Experimental

4.1. General methods

Melting points were uncorrected. The IR spectra were recorded as Nujol mulls with a Bruker IFS 66 spectrophotometer. The 1H and ${}^{13}C$ NMR spectra ($CDCl_3$, DMSO or CD_3OD , internal Me_4Si) were measured with a Bruker Avance III 500 (500.13/125.75 MHz) instrument. Positive-ion mode MALDITOF mass spectra were obtained using a Bruker Biflex III spectrometer with 4-cyano-4-hydroxycinnamic matrix. The optical rotations were determined at rt on a Perkin-Elmer polarimeter in a 1-dm tube at the D line of sodium using $CHCl_3$ or CH_3OH as the solvents. Thin-layer chromatography (TLC) was performed on the E. Merc Kieselgel 60 F-254 plates using the following eluent systems (v/v): A, 2:1 toluene-AcOEt; B, 4:1 toluene-AcOEt; C, 3:1 $CHCl_3$ -MeOH; D, 6:1 $CHCl_3$ -MeOH. Column chromatography was performed on MN Kieselgel 60 (<0.08 mm) with one of the above listed eluent systems.

4.2. Benzyl 3,4,6-tri-O-acetyl-2-deoxy-(2E)-hydroxyimino-β-D-arabino- (3) -(2Z)-hydroxyimino-α-D-arabino- (4) and -(2Z)-hydroxyimino-β-D-arabino-hexopyranosides (5)

3,4,6-Tri-O-acetyl-2-deoxy-2-nitroso-α-D-glucopyranosyl chloride (**1**) (0.34 g, 1 mmol) [37], benzyl alcohol (208 μL, 2 mmol), and dry pyridine (161 μL, 2 mmol) were dissolved in anhydrous THF (7.5 mL). The reaction mixture was stirred and refluxed for 0.5 h. The end of reaction was verified by TLC (solvent A). Then, the mixture was evaporated, dissolved in CHCl₃ (100 mL), washed several times with H₂O (20 mL), dried over Na₂SO₄, filtered off and concentrated. The residue was chromatographed on silica gel (solvent B) to afford first **3** (34.9 mg, 9%, syrup): [α]_D²⁰ – 8° (c 1.0, CHCl₃); R_f 0.48 (solvent A); IR: ν 3375 (O–H), 3032 (Bn C–H), 2932 (C–H), 1749 (ester C=O), 1238 cm^{–1} (ester C–O); ¹H NMR (CDCl₃, 500 MHz): δ 7.83 (s, 1 H, NOH), 7.37 (m, 5 H, Ph), 6.11 (d, 1 H, J_{3,4} 7.4 Hz, H-3), 5.68 (dd, 1 H, J_{3,4} 7.55 Hz, J_{4,5} 8.8 Hz H-4), 5.22 (s, 1 H, H-1), 4.91 (d, 1 H, J_{A,B} 12.2 Hz, CH_APh), 4.67 (d, 1 H, J_{A,B} 12.05 Hz CH_BPh), 4.35 (dd, 1 H, J_{5,6} 4.7 Hz, J_{6,6'} 12.1 Hz, H-6), 4.24 (dd, 1 H, J_{5,6'} 3.45 Hz, J_{6,6'} 12.05 Hz, H-6'), 3.97 (m, 1 H, H-5), 2.04 (s, 6 H, 2 × OAc), 2.01 (s, 3 H, OAc); ¹³C NMR (CDCl₃, 125 MHz): δ 170.7, 169.7, 169.6 (3 × C=O), 149.4 (C2), 136.8, 128.5, 127.9, 127.7 (C_{arom}), 95.7 (C1), 71.8 (C5) 69.1 (CH₂), 68.1 (C4), 63.7 (C3), 63.1 (C6), 20.72, 20.7, 20.5 (3 × COCH₃); MALDI-TOF-MS: *m/z* 432.2 (M+Na)⁺ 448.1 (M+K)⁺.

Eluted second was **4** (188.9 mg, 46%, syrup): [α]_D²⁰ + 81° (c 1.0, CHCl₃); R_f 0.42 (solvent A); IR: ν 3375 (O–H), 3032 (Bn C–H), 2930 (C–H), 1754 (ester C=O), 1230 cm^{–1} (ester C–O); ¹H NMR (CDCl₃, 500 MHz): δ 8.11 (s, 1 H, NOH), 7.35 (m, 5 H, Ph), 6.08 (s, 1 H, H-1), 5.81 (d, 1 H, J_{3,4} 9.65 Hz, H-3), 5.20 (t, 1 H, J_{3,4} 9.65 Hz, J_{4,5} 9.8 Hz, H-4), 4.74 (d, 1 H, J_{A,B} 11.85 Hz, CH_APh), 4.67 (d, 1 H, J_{A,B} 11.85 Hz, CH_BPh), 4.28 (dd, 1 H, J_{5,6} 4.4 Hz, J_{6,6'} 12.35 Hz, H-6), 4.19 (ddd, 1 H, J_{4,5} 10.1 Hz, J_{5,6} 4.4 Hz, J_{5,6'} 2.2 Hz H-5), 4.02 (dd, 1 H, J_{5,6'} 2.4 Hz, J_{6,6'} 12.3 Hz H-6'), 2.08 (s, 3 H, OAc), 2.06 (s, 3 H, OAc), 2.04 (s, 3 H, OAc); ¹³C NMR (CDCl₃, 125 MHz): δ 170.7, 169.7, 169.3 (3 × C=O), 148.9 (C2), 136.4, 128.5, 128.2, 128.1 (C_{arom}), 89.8 (C1), 70.2 (CH₂), 69.5 (C3), 69.3 (C4), 68.0 (C5), 61.8 (C6), 20.7, 20.6, 20.5 (3 × COCH₃); MALDI-TOF-MS: *m/z* 432.2 (M+Na)⁺, 448.1 (M+K)⁺.

Eluted third was **5** (32.9 mg, 8%, syrup): R_f 0.39 (solvent A); IR: ν 3344 (O–H), 2958, 2928 (C–H), 1747 (ester C=O), 1658 (C=N), 1230 cm^{–1} (ester C–O); ¹H NMR (CDCl₃, 500 MHz): δ 8.12 (s, 1 H, NOH), 7.34 (m, 5 H, Ph), 5.88 (s, 1 H, H-1), 5.52 (d, 1 H, J_{3,4} 5.5 Hz, H-3), 5.31 (t, 1 H, J_{3,4} 5.5 Hz, J_{4,5} 5.5 Hz, H-4), 4.91 (d, 1 H, J_{A,B} 12.2 Hz, CH_APh), 4.69 (d, 1 H, J_{A,B} 12.2 Hz, CH_BPh), 4.43 (d, 2 H, J_{5,6} 6.1 Hz, 2 × H-6), 4.03 (q, 1 H, J_{4,5} 5.85 Hz, J_{5,6} 6.4 Hz, H-5), 2.08 (s, 3 H, OAc), 2.08 (s, 3 H, OAc), 2.07 (s, 3 H, OAc); ¹³C NMR (CDCl₃, 125 MHz): δ 170.6, 169.5, 169.4 (3 × C=O), 149.1 (C2), 136.7, 128.4, 128.0, 127.0 (C_{arom}), 90.2 (C1), 72.6 (C5), 70.6 (CH₂), 68.3 (C4), 68.1 (C3), 64.0 (C6), 20.84, 20.79 (3 × COCH₃); MALDI-TOF-MS: *m/z* 432.2 (M+Na)⁺, 448.2 (M+K)⁺.

4.3. Benzyl 3,4,6-tri-O-acetyl-2-deoxy-(2E)-hydroxyimino-β-D-lyxo- (6), -(2Z)-hydroxyimino-β-D-lyxo- (7) and -(2Z)-hydroxyimino-α-D-lyxo-hexopyranosides (8)

These were synthesized analogously to **3–5** using 3,4,6-tri-O-acetyl-2-deoxy-2-nitroso-α-D-galactopyranosyl chloride (**2**) (1 g, 3 mmol) [37], benzyl alcohol (615 μL, 6 mmol), pyridine (0.5 mL, 6 mmol) and THF (22.5 mL). Column chromatography (solvent B) gave first a mixture of **6** and **7** (131.3 mg 11%, syrup): R_f 0.40 (solvent A); IR: ν 3398 (O–H), 3030 (Bn C–H), 2937 (C–H), 1749 (ester C=O), 1230 cm^{–1} (ester C–O); ¹H NMR (CDCl₃, 500 MHz) for **6**: δ 8.06 (bs, 1 H, NOH), 7.27 (m, 5 H, Ph), 6.32 (d, 1 H, J_{3,4} 3.9 Hz, H-3), 5.19 (s, 1 H, H-1), 5.17 (t, 1 H, J_{3,4} 4.3 Hz, J_{4,5} 4.65 Hz, H-4), 4.85 (d, 1 H, J_{A,B} 11.5 Hz, CH_APh), 4.69 (dd, 1 H, J_{5,6} 8.75 Hz, J_{6,6'} 11.95 Hz, H-

6), 4.57 (d, 1 H, J_{A,B} 11.5 Hz, CH_BPh), 4.47 (dd, 1 H, J_{5,6'} 3.8 Hz, J_{6,6'} 11.95 Hz, H-6'), 4.21 (m, 1 H, H-5), 2.02, 2.01, 1.96 (3 s, 9 H, 3 × OAc); ¹³C NMR (CDCl₃, 125 MHz): δ 170.8, 169.8, 169.7 (3 × C=O), 148.4 (C2), 136.1, 128.5, 127.9 (C_{arom}), 96.1 (C1), 71.4 (C5), 69.1 (CH₂), 67.0 (C4), 63.9 (C6), 60.6 (C3), 20.9, 20.8, 20.6 (3 × COCH₃); for **7**: δ 8.06 (bs, 1 H, NOH), 7.27 (m, 5 H, Ph), 5.79 (s, 1 H, H-1), 5.73 (d, 1 H, J_{3,4} 3.35 Hz, H-3), 5.39 (dd, 1 H, J_{3,4} 3.4 Hz, J_{4,5} 5.8 Hz, H-4), 4.87 (d, 1 H, J_{A,B} 11.5 Hz, CH_APh), 4.63 (d, 1 H, J_{A,B} 11.5 Hz, CH_BPh), 4.56 (dd, 1 H, J_{5,6} 8.7 Hz, J_{6,6'} 11.6 Hz, H-6), 4.41 (dd, 1 H, J_{5,6'} 4.75 Hz, J_{6,6'} 11.6 Hz, H-6'), 4.31 (m, 1 H, H-5), 2.02, 2.01, 2.00 (3 s, 9 H, 3 × OAc); ¹³C NMR (CDCl₃, 125 MHz): δ 170.7, 169.7, 169.8 (3 × C=O), 149.1 (C2), 136.8, 128.4, 127.8 (C_{arom}), 91.1 (C1), 71.8 (C5), 70.6 (CH₂), 67.3 (C3), 67.2 (C4), 63.6 (C6), 20.9, 20.7 (3 × COCH₃); MALDI-TOF-MS: *m/z* 432.2 (M+Na)⁺, 448.1 (M+K)⁺.

Eluted second was **8** (519 mg, 42%, syrup): [α]_D²⁰ + 66.0° (c 1.0, CHCl₃); R_f 0.35 (solvent A); IR: ν 3354 (O–H), 3031 (Bn C–H), 2932 (C–H), 1750 (ester C=O), 1230 cm^{–1} (ester C–O); ¹H NMR (CDCl₃, 500 MHz): δ 8.76 (bs, 1 H, NOH), 7.35 (m, 5 H, Ph), 6.13 (s, 1 H, H-1), 5.89 (d, 1 H, J_{3,4} 3.4 Hz, H-3), 5.50 (d, 1 H, J_{3,4} 3.2 Hz H-4), 4.76 (d, 1 H, J_{A,B} 11.75 Hz, CH_APh), 4.65 (d, 1 H, J_{A,B} 11.75 Hz, CH_BPh), 4.43 (t, 1 H, J_{5,6} 6.6 Hz, J_{5,6'} 6.55 Hz H-5), 4.09 (d, 1 H, J_{5,6} 6.6 Hz, H-6), 4.08 (d, 1 H, J_{5,6'} 6.55 Hz, H-6'), 2.13 (s, 3 H, OAc), 2.08 (s, 3 H, OAc), 2.07 (s, 3 H, OAc); ¹³C NMR (CDCl₃, 125 MHz): δ 170.4, 170.3, 169.4 (3 × C=O), 147.7 (C2), 136.4, 128.5, 128.2, 128.1 (C_{arom}), 89.7 (C1), 70.1 (CH₂), 69.1 (C4), 67.1 (C5), 66.9 (C3), 61.7 (C6), 20.7, 20.6, 20.4 (3 × COCH₃); MALDI-TOF-MS: *m/z* 432.2 (M+Na)⁺, 448.1 (M+K)⁺.

4.4. General procedure for O-deacetylation

The mixture of **3**, **4**, or **7** (40.9 mg, 0.1 mmol) and 0.1 M solution of MeONa in MeOH (0.6 mL, 0.06 mmol) was stirred at rt for 0.5 h. The end of reaction was verified with TLC (solvent C). Then, it was treated with Dowex H⁺ 50WX4-400, filtered and concentrated.

4.4.1. Benzyl 2-deoxy-(2E)-hydroxyimino-β-D-arabino-hexopyranoside (9)

Deacetylation of **3** (51.1 mg, 0.12 mmol) gave **9** (35.3 mg, 99%, mp 150–151 °C): [α]_D²⁰ – 23.0 (c 0.8, CH₃OH); R_f 0.8 (solvent C); IR: ν 3462, 3359 (O–H), 3074 (Bn C–H), 2919 (C–H), 1628 (C=N); ¹H NMR (CD₃OD, 500 MHz): δ 7.35 (m, 5 H, Ph), 5.14 (s, 1 H, H-1), 4.86 (d, 1 H, J_{A,B} 11.75 Hz, CH_APh), 4.63 (d, 1 H, J_{A,B} 11.75 Hz, CH_BPh), 4.57 (d, 1 H, J_{3,4} 8.2 Hz, H-3), 4.21 (dd, 1 H, J_{3,4} 8.6 Hz, J_{4,5} 9.4 Hz, H-4), 3.87 (dd, 1 H, J_{6,6'} 11.7 Hz, J_{5,6'} 2.8 Hz H-6'), 3.75 (dd, 1 H, J_{5,6} 5.6 Hz, J_{6,6'} 11.7 Hz, H-6), 3.49 (ddd, 1 H, J_{4,5} 9.4 Hz, J_{5,6} 5.6 Hz, J_{5,6'} 2.8 Hz, H-5); ¹³C NMR (CD₃OD, 125 MHz): δ 153.1 (C2), 137.7, 127.9, 127.7, 127.2 (C_{arom}), 96.7 (C1), 76.8 (C5), 68.5 (CH₂), 68.4 (C4), 67.3 (C3), 62.6 (C6); MALDI-TOF-MS: *m/z* 284.3 (M+H)⁺, 306.1 (M+Na)⁺, 322.1 (M+K)⁺.

4.4.2. Benzyl 2-deoxy-(2E)-hydroxyimino-α-D-arabino- (10) and -(2Z)-hydroxyimino-α-D-arabino-hexopyranosides (11)

Deacetylation of **4** (211.3 mg, 0.5 mmol) gave a mixture of two products, which was chromatographed (solvent D) yielded first **10** (33.3 mg, 23%, syrup): R_f 0.8 (solvent C); IR: ν 3388, 3252 (O–H), 2927, 2878 (C–H), 1640 (C=N); ¹H NMR (CD₃OD, 500 MHz): δ 7.35 (m, 5 H, Ph), 6.16 (s, 1 H, H-1), 5.04 (d, 1 H, J_{3,4} 9.45 Hz, H-3), 4.81 (d, 1 H, J_{A,B} 11.5 Hz, CH_APh), 4.65 (d, 1 H, J_{A,B} 11.8 Hz, CH_BPh), 3.88 (m, 1 H, H-5), 3.74 (m, 1 H, H-4); ¹³C NMR (CD₃OD, 125 MHz): δ : 137.3, 127.9, 127.7, 127.5 (C_{arom}), 90.3 (C1), 82.2 (C3), 72.9 (C5), 69.7 (C4), 68.9 (CH₂), 60.9 (C6); MALDI-TOF-MS: *m/z* 306.1 (M+Na)⁺, 322.1 (M+K)⁺.

Eluted second was **11** (69 mg, 47%, mp 108 °C): [α]_D²⁰ + 131.8° (c 1, CH₃OH); R_f 0.64 (solvent C); IR: ν 3388, 3244 (O–H), 2928 (C–H), 1641 (C=N); ¹H NMR (CD₃OD, 500 MHz): δ 7.35 (m, 5 H, Ph), 6.10 (s, 1 H, H-1), 4.80 (d, 1 H, J_{A,B} 11.75 Hz, CH_APh), 4.63 (d, 1 H, J_{A,B} 11.75 Hz,

CH_BPh), 4.36 (d, 1 H, *J*_{3,4} 9.25 Hz, H-3), 3.87 (dd, 1 H, *J*_{5,6'} 2.0 Hz, *J*_{6,6'} 11.7 Hz, H-6'), 3.81 (ddd, 1 H, *J*_{4,5} 9.6 Hz, *J*_{5,6} 5.7 Hz, *J*_{5,6'} 2.0 Hz, H-5), 3.73 (dd, 1 H, *J*_{5,6} 5.7 Hz, *J*_{6,6'} 11.7 Hz, H-6), 3.41 (t, 1 H, *J*_{3,4} 9.25 Hz, *J*_{4,5} 9.6 Hz, H-4); ¹³C NMR (CD₃OD, 125 MHz): δ 152.5 (C2), 137.4, 128.0, 127.8, 127.4 (C_{arom}), 89.6 (C1), 73.0 (C4), 72.7 (C5), 71.3 (C3), 68.9 (CH₂), 61.1 (C6); MALDITOF-MS: *m/z* 306.1 (M+Na)⁺, 322.1 (M+K)⁺.

4.4.3. Benzyl 2-deoxy-(2Z)-hydroxyimino-α-D-lyxo-hexopyranoside (12)

Deacetylation of **8** (776.8 mg, 1.9 mmol) gave **12** (362.7 mg, 68%, mp 155 °C): [α]_D²⁰ +188.7° (c 1, CH₃OH); *R*_f 0.65 (solvent C); IR: ν 3379 (O–H), 2950, 2922, 2900 (C–H), 1641 (C=N); ¹H NMR (CD₃OD, 500 MHz): δ 7.34 (m, 5 H, Ph), 6.10 (s, 1 H, H-1), 4.81 (d, 1 H, *J*_{A,B} 11.75 Hz, CH_APh), 4.63 (d, 1 H, *J*_{A,B} 11.75 Hz, CH_BPh), 4.54 (d, 1 H, *J*_{3,4} 3.2 Hz, H-3), 4.07 (t, 1 H, *J*_{5,6} 6.4 Hz, *J*_{5,6'} 5.6 Hz, H-5), 4.03 (d, 1 H, *J*_{3,4} 3.2 Hz, H-4), 3.76 (dd, 1 H, *J*_{5,6} 6.4 Hz, *J*_{6,6'} 11.4 Hz, H-6), 3.72 (dd, 1 H, *J*_{5,6'} 5.6 Hz, *J*_{6,6'} 11.4 Hz, H-6'); ¹³C NMR (CD₃OD, 125 MHz): δ 151.5 (C2), 137.4, 127.9, 127.8, 127.4 (C_{arom}), 89.7 (C1), 71.4 (C5), 70.9 (C4), 68.9 (CH₂), 68.3 (C3), 61.3 (C6); MALDITOF-MS: *m/z* 284.1 (M+H)⁺, 306.1 (M+Na)⁺.

4.5. Description of the crystal structure of 12

Good-quality single-crystal specimen was selected for the X-ray diffraction experiments at *T* = 295(2) K and affixed to the tip of glass capillary with epoxy glue. Diffraction data were obtained on the Oxford Diffraction Gemini R Ultra Ruby CCD diffractometer, using a MoKα radiation source (*λ* = 0.71073 Å). The lattice parameters were obtained by least-squares fit to the optimized setting angles of the reflections by means of *CrysAlis CCD* [38]. Data were reduced using *CrysAlis RE* software [38]. The structural resolution procedure was carried out with the *SHELXS-97* package [39], solving the structure by direct methods and carrying out refinements by full-matrix least-squares on *F*² using the *SHELXL-97* program [39]. The H-atoms at hydroxyl O-atoms were located on a Fourier-difference map, recalculated in their ideal positions with O–H = 0.82 Å and constrained to ride on their parent atom with *U*_{iso}(H) = *xU*_{eq}(O), where *x* = 1.5. Other H-atoms were positioned geometrically, with C–H = 0.93 Å and 0.98 Å for the aromatic and methylene H-atoms, respectively, and constrained to ride on their parent atoms with *U*_{iso}(H) = 1.2 *U*_{eq}(C).

The crystal structure was refined to *R*₁ = 0.0294 (2361 reflections, all unique reflections) and *R*₁ = 0.0274 (2250 reflections with *F* > 2σ(*F*₀)) by full-matrix least-squares method using the program *SHELXL-97* [39] based on 181 parameters. The compound structure showing the atom numbering system is illustrated in Fig. 1. Molecular packing in the crystal, illustrated in Fig. 2, was prepared by *ORTEP-3* program [40]. The computational material for publication was prepared using the *PLATON* program [36].

4.6. Methods used in DFT studies on methyl 2-deoxy-2-hydroxyimino-D-hexopyranosides

All the calculated structures were prepared in the MOLDEN program [41]. A full geometry optimisation was conducted using density functional theory (DFT) based on Becke's three-parameter hybrid exchange functional involving the gradient-corrected correlation functional of Lee, Yang and Parr, with the split-valence basis set including polarized and diffuse functions (B3LYP/6-311+G** method) [42–44]. The convergence of all the systems studied was checked by calculating the harmonic vibrational frequencies at the same level. No imaginary frequencies were observed. All calculations were done under default conditions with the aid of the Gaussian 03 program [45].

The populations of the respective rotamers were calculated using Equation (1):

$$P_i = \frac{e^{-\Delta G_i/RT}}{\sum_{i=1}^N e^{-\Delta G_i/RT}} \quad (1)$$

Acknowledgements

This research was financed by the Ministry of Science and Higher Education – Grant DS/530-8457-D603-16. All DFT calculations were carried out using the resources of the Informatics Center of the Metropolitan Academic Network in Gdańsk (CI TASK).

Supplementary data

Full crystallographic details, excluding structures features, have been deposited (deposition No. CCDC 1443825) with the Cambridge Crystallographic Data Center. These data may be obtained, on request, from The Director, CCDC, 12 Union Road, Cambridge, CB2 1EZ, UK (tel.: +44-1223-336408; fax: +44-1223-336033; e-mail: deposit@ccdc.cam.ac.uk or [www: http://www.ccdc.cam.ac.uk](http://www.ccdc.cam.ac.uk)).

References

- [1] R.U. Lemieux, T.L. Nagabhushan, S.W. Gunner, *Can. J. Chem.* 46 (1968) 405–413.
- [2] F.W. Lichtenthaler, E. Kaji, S. Weprek, *J. Org. Chem.* 50 (1985) 3505–3515.
- [3] F.W. Lichtenthaler, *Chem. Rev.* 111 (2011) 5569–5609.
- [4] R.U. Lemieux, F.Z.G. Georges, Z. Smiatcz, *Can. J. Chem.* 59 (1981) 1433–1438.
- [5] B. Liberek, Z. Smiatcz, *J. Carbohydr. Chem.* 19 (2000) 1259–1267.
- [6] R.U. Lemieux, T.L. Nagabhushan, *Can. J. Chem.* 46 (1968) 401–405.
- [7] K. Miyai, R.W. Jeanloz, *Carbohydr. Res.* 21 (1972) 45–55.
- [8] E. Kaji, N. Anabuki, S. Zen, *Chem. Pharm. Bull.* 43 (1995) 1441–1447.
- [9] M. Kugelman, A.K. Mallams, H.F. Vernay, D.F. Crowe, M. Tanabe, *J. Chem. Soc. Perkin Trans. 1* (1976) 1088–1097.
- [10] H. Paulsen, P. Stadler, F. Tödter, *Chem. Ber.* 110 (1977) 1925–1930.
- [11] W. Karpiesiuk, A. Banaszek, *Carbohydr. Res.* 299 (1997) 245–252.
- [12] A. Veit, B. Giese, *SYNLETT* 3, 1990, p. 166.
- [13] E. Kaji, F.W. Lichtenthaler, *Trends Glycosci. Glycotechnol.* 5 (1993) 121–142.
- [14] A. Banaszek, W. Karpiesiuk, *Carbohydr. Res.* 251 (1994) 233–242.
- [15] P.L. Barili, G. Berti, G. Catelani, F. D'Andrea, V. Di Bussolo, *Carbohydr. Res.* 290 (1996) 17–31.
- [16] J.J. Gridley, H.M.I. Osborn, *J. Chem. Soc. Perkin Trans. 1* (2000) 1477–1491.
- [17] R.U. Lemieux, R.A. Earl, K. James, T.L. Nagabhushan, *Can. J. Chem.* 51 (1973) 19–26.
- [18] P. Jarglis, V.H. Göckel, F.W. Lichtenthaler, *Tetrahedron Asymmetry* 20 (2009) 952–960.
- [19] M. Brehm, H. Volker, V.H. Göckel, P. Jarglis, F.W. Lichtenthaler, *Tetrahedron Asymmetry* 19 (2008) 358–373.
- [20] M. Lergenmüller, U. Kläres, F.W. Lichtenthaler, *Carbohydr. Res.* 344 (2009) 2127–2136.
- [21] P.M. Collins, W.G. Overend, *J. Chem. Soc.* (1965) 3448–3456.
- [22] A. Melcer, I. Łącka, I. Gabriel, M. Wojciechowski, B. Liberek, A. Wiśniewski, S. Milewski, *Bioorg. Med. Chem. Lett.* 17 (2007) 6602–6606.
- [23] S. Milewski, *Biochim. Biophys. Acta* 1597 (2002) 173–192.
- [24] M.M.A. Pereira, P.P. Santos, Rearrangements of hydroxylamines, oximes, and hydroxamic acids, in: Z. Rappoport, J.F. Liebman (Eds.), *The Chemistry of Hydroxyl- Amines, Oximes, and Hydroxamic Acids*, Vol. 1, Wiley, New York, 2009, p. 343.
- [25] D.S. Bohle, Z. Chua, I. Perepichka, K. Rosadiuk, *Chem. Eur. J.* 19 (2013) 4223–4229.
- [26] B. Liberek, A. Sikorski, A. Melcer, A. Konitz, *Carbohydr. Res.* 338 (2003) 795–799.
- [27] B. Liberek, A. Konitz, R. Frankowski, Z. Smiatcz, *Carbohydr. Res.* 326 (2000) 151–158.
- [28] T. Nakagawa, F.W. Lichtenthaler, *Tetrahedron Asymmetry* 22 (2011) 740–744.
- [29] A. Nowacki, B. Liberek, *J. Phys. Chem. A* 112 (2008) 7072–7079.
- [30] A. Nowacki, D. Walczak, B. Liberek, *Carbohydr. Res.* 352 (2012) 177–185.
- [31] A. Nowacki, H. Myszk, B. Liberek, *Carbohydr. Res.* 377 (2013) 4–13.
- [32] ChB. Aakeröy, A.S. Sinha, K.N. Epa, P.D. Chopade, M.M. Smith, *J. Desper, Cryst. Growth Des.* 13 (2013) 2687–2695.
- [33] G.G. Evans, J.A. Boeyens, *Acta Cryst. B45* (1989) 581–590.
- [34] W. Saenger, *Principles of Nucleic Acid Structure*, Springer, New York, 1983, p. 19.

- [35] D. Cremer, J.A. Pople, *J. Am. Chem. Soc.* 97 (1975) 1354–1358.
- [36] A.L. Spek, *Acta Cryst. D* 65 (2009) 148–155.
- [37] R.U. Lemieux, T.L. Nagabhushan, I.K. O'Neill, *Can. J. Chem.* 46 (1968) 413–418.
- [38] Oxford Diffraction, *CrysAlis CCD and CrysAlis RED*, Oxford Diffraction Ltd, Yarnton, Oxfordshire, England, 2008.
- [39] G.M. Sheldrick, *Acta Cryst. Sect. A* 64 (2008) 112–122.
- [40] L.J. Farrugia, *J. Appl. Cryst.* 30 (1997) 565.
- [41] G. Schaftenaar, J.H. Noordik, *J. Comput.-Aided Mol. Des.* 14 (2000) 123–134.
- [42] A.D. Becke, *J. Chem. Phys.* 98 (1993) 5648–5652.
- [43] C. Lee, W. Yang, R.G. Parr, *Phys. Rev. B* 37 (1988) 785–789.
- [44] J.-L.M. Abboud, O. Castaño, J.Z. Dávalos, P. Jiménez, R. Gomperts, P. Müller, M.V. Roux, *J. Org. Chem.* 67 (2002) 1057–1060.
- [45] M.J. Frisch, G.W. Trucks, H.B. Schlegel, G.E. Scuseria, M.A. Robb, J.R. Cheeseman, J.A. Montgomery Jr., T. Vreven, K.N. Kudin, J.C. Burant, J.M. Millam, S.S. Iyengar, J. Tomasi, V. Barone, B. Mennucci, M. Cossi, G. Scalmani, N. Rega, G.A. Petersson, H. Nakatsuji, M. Hada, M. Ehara, K. Toyota, R. Fukuda, J. Hasegawa, M. Ishida, T. Nakajima, Y. Honda, O. Kitao, H. Nakai, M. Klene, X. Li, J.E. Knox, H.P. Hratchian, J.B. Cross, V. Bakken, C. Adamo, J. Jaramillo, R. Gomperts, R.E. Stratmann, O. Yazyev, A.J. Austin, R. Cammi, C. Pomelli, J.W. Ochterski, P.Y. Ayala, K. Morokuma, G.A. Voth, P. Salvador, J.J. Dannenberg, V.G. Zakrzewski, S. Dapprich, A.D. Daniels, M.C. Strain, O. Farkas, D.K. Malick, A.D. Rabuck, K. Raghavachari, J.B. Foresman, J.V. Ortiz, Q. Cui, A.G. Baboul, S. Clifford, J. Cioslowski, B.B. Stefanov, G. Liu, A. Liashenko, P. Piskorz, I. Komaromi, R.L. Martin, D.J. Fox, T. Keith, M.A. Al-Laham, C.Y. Peng, A. Nanayakkara, M. Challacombe, P.M.W. Gill, B. Johnson, W. Chen, M.W. Wong, C. Gonzalez, J.A. Pople, *Gaussian 03; Revision C.02*, Gaussian, Inc., Pittsburgh, PA, 2004.